The effect of changing disk parameters on whirling frequency of high speed rotor system

A M Abdul Wahab, Z A Rasid*, A Abu, N F Mohd Noor Rudin and F Yakub

Malaysia-Japan International Institute of Technology, Universiti Teknologi Malaysia, Kuala Lumpur, Malaysia.

*arzainudin.kl@utm.my

Abstract. The requirement for efficiency improvement of machines has caused machine rotor to be designed to rotate at high speeds. It is known that whirling natural frequency of a shaft changes with the change of shaft speed and the design needs to avoid points of resonance where the whirling frequency equals the shaft speed. At high speeds, a shaft may have to carry a huge torque along and this torsional effect has been neglected in past shaft analyses. Whirling behaviour of high speed rotating shaft is investigated in this study with consideration of the torsional effect of the shaft. The shaft system under study consists of a shaft, discs and two bearings, and the focus is on the effect of the disc parameters. A finite element formulation is developed based on Nelson's 5 degrees of freedom (DOF) per node element that includes the torsional degree of freedom. Bolotin's method is applied to the derived Mathieu-Hill type of equation to get quadratic eigenvalues problem that gives the forward and backward frequencies of the shaft. Campbell's diagrams are drawn in studying the effect of discs on the whirling behaviour of the shaft. It is found that the addition of disks on the shaft decreases the whirling frequency of the shaft and the frequency is lower for mass located at the centre of the shaft compared to the one located near to the end. The effect of torsional motion is found to be significant where the difference between critical speed of 4DOF and 5DOF models can be as high as 15%.

1. Introduction

Vibration control is one of the main concerns in the design of rotating shaft. The demand of the market today for more powerful and efficient rotating machines has led to the design of machines that need to be operated at high speeds [1]. Classification of high speed rotating equipment lies in between 10000 RPM and 100000 RPM [2]. Such rotating equipment that operates at high speed has been used in wide ranges of industrial applications like textile [3], automotive [4] and electrical spindle [5]. An important type of vibration that needs to be controlled is the lateral vibration, which is called whirling. Whirling is a phenomenon where the plane of the enclosed bent up shaft–axis and the bearing centre line rotates about the bearing centre line, causing the shaft to bow out as illustrated in Figure 1. This condition can occur due to the mass imbalance of the shaft or disks and it occurs at resonance where whirling natural frequency is equal to the spin speed. Due to the gyroscopic effect of the shaft, whirling frequency is known to not only split into two but also changes with the spin speed. The frequency might increase with speed as the shaft whirls in the rotational direction of the shaft and this frequency is called the forward frequency (FF). In opposite manner, the shaft whirls in direction opposite to the shaft rotation while this backward frequency (BF) decreases with the spin speed. This behavior is usually captured in

Content from this work may be used under the terms of the Creative Commons Attribution 3.0 licence. Any further distribution of this work must maintain attribution to the author(s) and the title of the work, journal citation and DOI.
Published under licence by IOP Publishing Ltd

the Campbell diagram as shown in Figure 2. Resonance occurs at point R where the FF is equal to the spin speed. The spin speed at resonance is called the critical speed, Ω_{cr}. To avoid this resonance condition that may occur when this changing frequency of the shaft equals the shaft speed, it is very important for accurate modal analysis to be conducted in the rotor system.

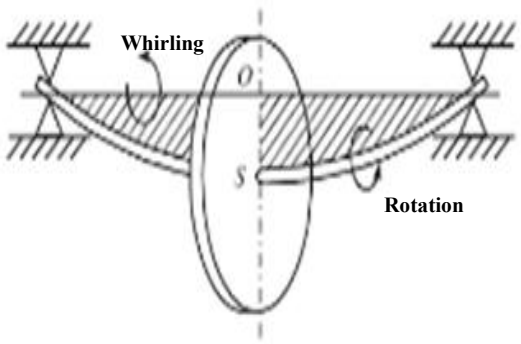

Figure 1: The whirling of a shaft [6]

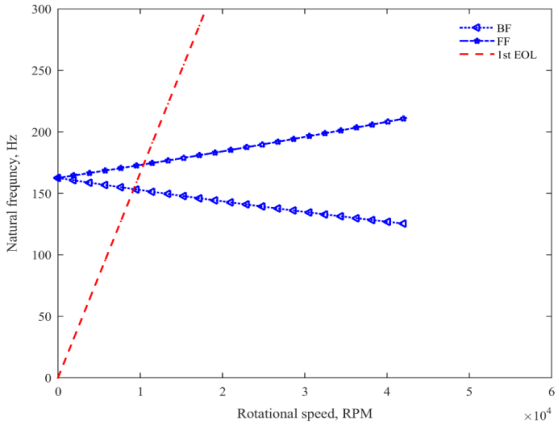

Figure 2: The Campbell diagram of a shaft

Lien-Wen and Der-Ming (1991) [7] applied the three-nodal, C^0 Timoshenko beam finite element model to investigate natural whirl speeds of rotating shaft with various end conditions and slenderness ratios. Effects of translational and rotary inertia, gyroscopic moments, bending and shear deformation are included in the mathematical model. The numerical results of the study indicated that the natural whirl speeds are considerably affected by the end conditions of the rotating shafts, shear deformation and the rotary inertia. In a different method of analysis, free vibrations of shafts supported on resilient bearings have been analyzed by Karunendiran and Zu (1999) [8]. Using Timoshenko beam theory, the exact frequency equation in the complex compact form is derived. The rotary inertia and gyroscopic effects are included while shear deformation effect is neglected. Meanwhile, a study on free vibration of a simply supported rotating shaft with stretching nonlinearity has been conducted by Hosseini and Zamanian (2013) [9]. The equations of motion are derived with the aid of the Hamilton principle and then transformed to the complex form. To analyze the free vibration, the method of multiple scales is directly applied to the partial differential equation of motion. It has been shown in that study that both forward and backward nonlinear natural frequencies are being excited. Furthermore, another study has stated that the forward and backward whirling modes are involved in investigating the free nonlinear vibrations of nonlinear slender rotating shaft [10]. It is found that the values of nonlinear forward and backward frequencies are lower in the second mode compared to first mode. 3D finite element-based model order reduction method has also been used to show the split of the sole resonant peak in case of gravity and unbalance condition due to anisotropy of bearings [11]. In addition, a cluster of additional resonant peaks appeared as both shaft and bearing are anisotropic. In rather complete modal analysis of a high speed rotor, Jalali et al. (2014) [12] used both 3D and 1D finite element method (FEM) to model the shaft. The natural frequencies and mode shapes of the rotor at rest under free–free boundary conditions are obtained, and the results are then compared to those obtained from the modal test. The Campbell diagram and the critical speeds are calculated using both FE models to evaluate the rotating system dynamics. The imbalance response of the system to the center of mass imbalance at the turbine is also calculated to investigate the dynamic behavior more practically and to verify the critical speeds obtained from the FEM.

The above studies show the progress in research on the characteristics of whirling frequencies of a shaft. However, except for Ref. [12], no other study has focused on high speed rotating shaft. At high rotating speed, a shaft may also carry high torque but the effect of this torque on whirling frequency of the shaft has been hardly considered. In their work to investigate the importance of considering the torsional effect of the shaft, Seshendra and Rao (2012) [13] have studied the whirling characteristics of

a geared rotor system for combined torsional-lateral vibrations. The study demonstrated that the lateral motions interact significantly with the torsional degrees of freedom when the resonance frequencies are similar. As such, this study is aimed to investigate the torsional effect on the whirling frequency of high speed rotor system that consists of a shaft, discs and bearings. The main focus is on the effect of several disc parameters on the whirling behavior of the shaft. FE formulation based on the Nelson's finite element model [14] that considers the torsional effect is developed. The Bolotin's method [15] is applied to the derived Mathieu-Hill type of equation to get the quadratic eigenvalues problem equation that gives the forward and backward frequencies of the shaft for the Campbell's diagram to be plotted.

2. Material and Methods

Referring to Figure 3, the rotor system used in this study consists of a shaft, one or more discs and two bearings. Bearings are represented as the supports in Figure 3. d is the diameter of the shaft whereas t is the thickness of the disk. L is the length of the shaft while *l* is the distance of the disk from the left bearing. Furthermore, Table 1 shows the material properties and dimensions of the shaft and bearing components of the rotor system. Table 2, on the other hand, tabulates the material properties and also dimensions of the discs attached to the shaft.

This study employs FEM to estimate the whirling natural frequency of the rotating shaft system. The finite element formulation developed here is based on Rao (2011) [16] where Timoshenko beam theory and Nelson's FEM approach [14] that considers the torsional effect are applied. FEM model that applies 5 degrees of freedom (DOF) per node including the torsional DOF is called 5DOF model in comparison to 4DOF model that does not consider the torsional DOF. Derivation of the formulation is very similar to that for parametric instability problem of rotating shaft.

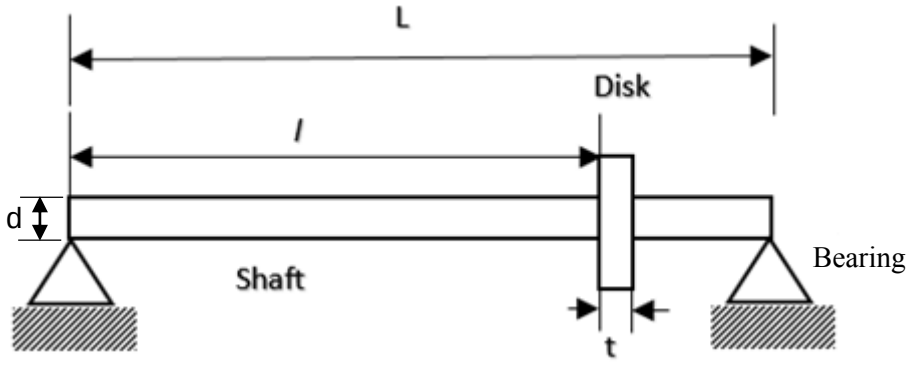

Figure 3: The rotor system being investigated

Table 1: Dimensions and material properties of the shaft and bearing of the rotor system

Shaft	
Young's modulus, E	207 GPa
Modulus of rigidity, G	79.6 GPa
Poisson's ratio, v	0.303
Density, ρ	7833 kg/m^3
Radius, r	round tube with r_{inner}= 0 m, r_{outer} =0.0508 m
Length, L	1.27 m
Shear factor, κ	0.9
Bearing	
Direct stiffness coefficient, K_{by},K_{bz}	7x10^7 N/m
Direct damping coefficient, C_{by},C_{bz}	0

Table 2: Dimensions and material properties of the disk correspond to the studies on the effect of the location of disc (Study 1), the mass of the disc (Study 2) and the number of discs attached (Study 3)

Disk in Study 1	
Young Modulus, *E*	207 GPa
Density, ρ	7833 kg/m^3
Thickness, t	0.03 m
Diameter, d	0.3 m
Disk in Study 2	
Young Modulus, *E*	207 GPa
Density, ρ	7833 kg/m^3
Diameter, d_1 and d_2	0.3 m
Thickness, nominal weight, t_1	0.03 m
Thickness, heavy weight, t_2	0.07 m
Diameter, d_3	0.16 m
Thickness, nominal weight, t_3	0.1055 m
Disk in Study 3	
Young Modulus, *E*	207 GPa
Density, ρ	7833 kg/m^3
Diameter, d_1, d_2	0.4 m
Thickness, t_1, t_2	0.005 m
Diameter, d_3	0.4 m
Thickness, t_3	0.006 m

Both types of whirling and the dynamic instability problem require the derivation of Mathiew-Hill equation such as in Equation 1, where $[M]$, $[G]$, $[K]$ and $[K_g]$ are the elemental mass, gyroscopic, stiffness and geometric stiffness matrices, respectively, Ω is the spin speed, $P(t)$ is the periodic axial force, α is the static load factor, β is the dynamic load factor and ϕ is the excitation frequency.

$$[M]\{\ddot{q}\} + \Omega[G]\{\dot{q}\} + ([K] - [K_g](\alpha P^* + \beta P^* \cos \phi T(t))\{q\} = 0 \quad (1)$$

Applying Bolotin's method [16], an infinite eigenvalues problem can be derived such as in Equation 2, which actually represents the whirling frequency problem to be solved in this study.

$$(\phi^2[M_E] + \phi[G_E] + [K_E])q = 0 \quad (2)$$

3. Results and Discussion

The effect of attaching disk to shaft on the whirling frequency of the shaft is investigated. In reference to Table 2, the effect of disk considered in this study constitutes of the effect of disk location with respect to shaft (Study 1), disk mass (Study 2) and disk number (Study 3) on the whirling frequency of the shaft.

Four cases are being compared here: Case 1 - shaft without any disk (no disk), Case 2 – shaft with a disk located at the middle of the shaft (disk @ 50%), Case 3 – shaft with a disk positioned near to the end of the shaft (disk @ 75%) and Case 4 – shaft with a disk positioned at the other end of the shaft with bearing inboard that results in overhung rotor (overhung). Disks with similar properties are used throughout the analysis as given in Table 2. The results from Case 1 are used as the benchmark for any differences that may occur in dynamic behaviour of the shaft when the disk is added. Rigid bearings are used in this study. Table 3 and Table 4 show the first and second modes of natural frequencies of static shaft for both 4DOF and 5DOF models, respectively. For the first mode, as tabulated in Table 3, the natural frequency for Case 2 is somewhat lower compared to that in Case 3. It should also be noted that, for the case of disk @ 75%, the disk is very near to the end of shaft where the radius of gyration of the shaft is smaller compared to that of the shaft with disk @ 50%. The reduction of the radius of gyration has decreased the moment of inertia of the disk. As a result, the natural frequency of the shaft is increased.

Table 3: First mode natural frequency of static shaft system for different disk locations

Disk location from end	Natural frequency, Hz 4DOF	Natural frequency, Hz 5DOF	Differences (%)
No disk	91.15	91.21	0.1
50%	79.94	79.98	0.1
75 %	83.34	83.38	0.0
Overhung	49.45	49.51	0.1

The opposite trend occurs to the second mode of frequency as the location of the disk changes. The natural frequency of disk in Case 2 of the shaft is higher than that in Case 3 such as shown in Table 4. For the case of overhung condition (Case 4), the natural frequencies are at the lowest for both first and second modes of frequency. This is because, in the overhung condition, the radius of gyration of the shaft is at its highest value. Thus the effect of moment of inertia of the disk that reduces the natural frequency is at its highest. On the other hand, in comparison between the 4DOF and 5DOF models, there is no significant effect of torsional motion on natural frequency of static shaft as the difference between the two models is only 0.3% at the highest. This occurs for both the first and second modes.

Table 4: Second mode natural frequency of static shaft system for different disk locations

Disk location from end	Natural frequency, Hz 4DOF	Natural frequency, Hz 5DOF	Differences (%)
No disk	203.62	204.16	0.3
50%	198.63	199.14	0.3
75 %	184.09	184.49	0.2
Overhung	157.17	157.42	0.2

Figure 4 and Figure 5 show the plots of first and second modes of vibration frequency against the rotational speed of the shaft, respectively, for the four cases of disk locations based on the 4DOF and 5DOF models. In general, the FF and BF natural frequencies are decreased for first and second modes as the disk is added to the shaft system. The effects of disk location on whirling speed for the first and second modes are shown in Table 5 and Table 6, respectively. It can be observed that the disk with overhung condition shows the smallest value of the critical speed, especially for the 5DOF model at 2865 RPM and 3084 RPM for BF and FF, respectively. As the disk is moved towards the end of the shaft, the whirling speed increases for both modes. This shows that the shaft with disk located near to its end can operate at a higher speed compared that with disk located far from the end. The effect of torsional motion considered in the 5DOF model is very significant. Both Figure 4 and Figure 5 show a big difference between the FF and BF natural frequencies of the 4DOF and 5DOF models. Similarly, critical speed differs for the 4DOF and 5DOF models, where the difference ranges from 2% to 8% as can be observed in Table 5 and Table 6. This shows that torsional motion needs to be considered in order to estimate accurately the whirling speed of rotating shaft with different locations of disk.

In the meantime, the effect of disk mass on the whirling frequency is also investigated here. A rotor with rigid bearings and centred single disk is used in this study. The comparison is between nominal disk, heavy disk and nominal thick disk to be attached to the shaft. While the masses of nominal disk and heavy disk differ, the mass of nominal disk and nominal thick disk is the same but the two differ in radius and thickness. Table 7 and Table 8 show the first and second modes of natural frequency of the shaft system, respectively.

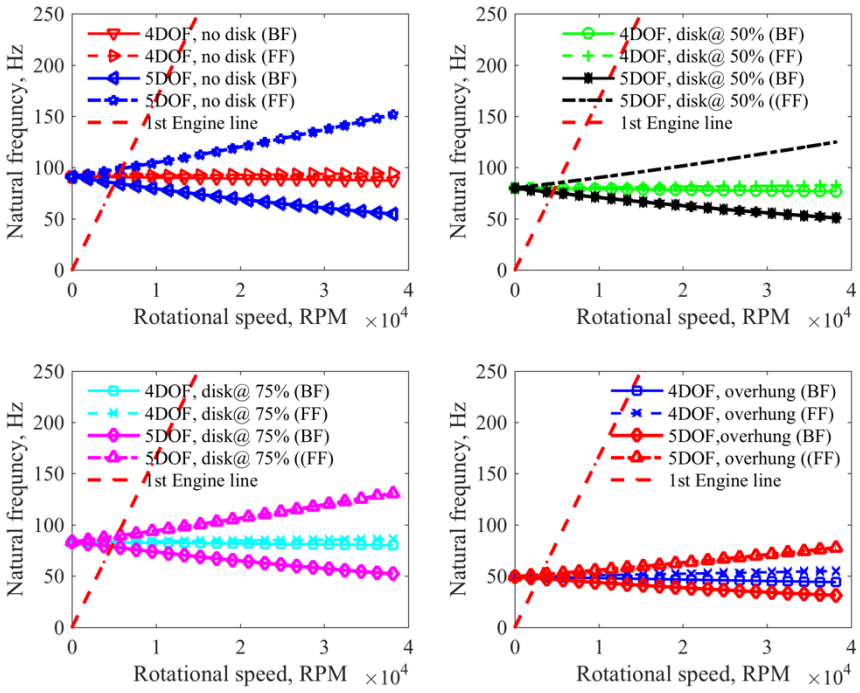

Figure 4: Effect of disk location on the whirling speed of shaft in the first mode

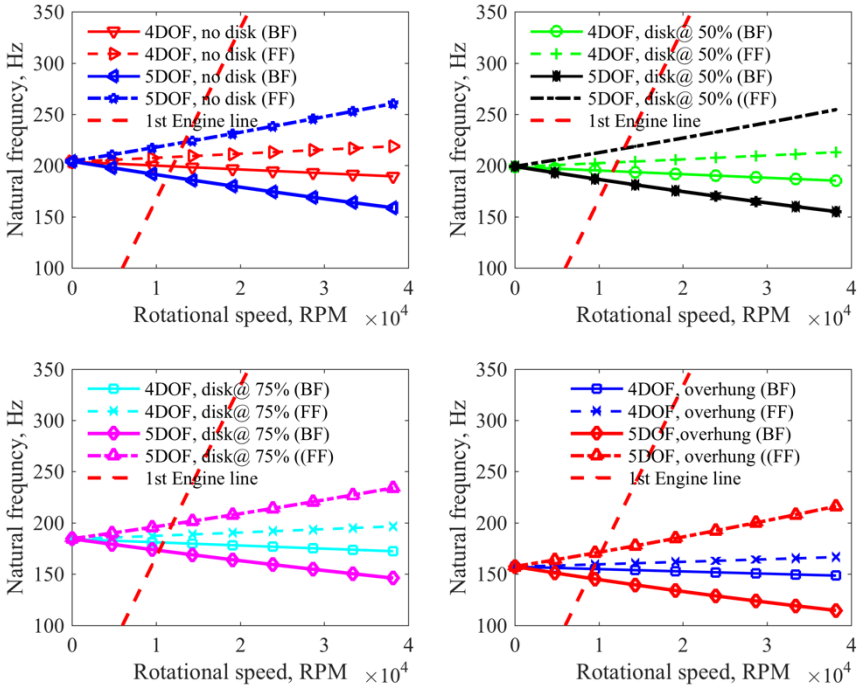

Figure 5: Effect of disk location on the whirling speed of shaft in the second mode

Table 5: Comparison of the first mode of whirling frequency for different disk locations

Disk location from end	Whirling direction	Whirling speed, RPM 4DOF	Whirling speed, RPM 5DOF	Differences, %
No disk	BF	5443	5099	-6.3
	FF	5500	5949	8.1
50 %	BF	4775	4545	-4.8
	FF	4822	5109	5.9
75 %	BF	4975	4708	-5.4
	FF	5023	5348	6.5
Overhung	BF	2960	2865	-3.2
	FF	2998	3084	2.9

Table 6: Comparison of the second mode of whirling frequency for different disk locations

Disk location from end	Whirling direction	Whirling speed, RPM 4DOF	Whirling speed, RPM 5DOF	Differences, %
No disk	BF	11940	11340	-5.0
	FF	12540	13380	6.7
50 %	BF	11690	11130	-4.8
	FF	12190	13020	6.8
75 %	BF	10840	10380	-4.2
	FF	11280	11960	6.0
Overhung	BF	9320	8785	-5.7
	FF	9597	10340	7.7

In Table 7, the first mode natural frequency of heavy disk is lower compared to that of the nominal disk in static condition. Table 7 also highlights that, since nominal disk and nominal thick disk have a similar mass, the natural frequencies for both conditions are similar. Similar results are obtained for the second mode of frequency of the shaft when the comparison is made between the nominal and the heavy disks such as shown in Table 8. However, in contrast to the case of the first mode, the second mode of natural frequency for nominal thick disk is higher than that of the nominal disk. For the first and second modes of the nominal and heavy disks, the mass of the disk might increase but the mass moment of inertia is unchanged because of their similar radius of gyration. Thus the natural frequency decreases as the mass increases. Similar condition occurs for the nominal and nominal thick disks that have the same mass in the first mode. With similar mass and unchanged mass moment of inertia, the natural frequencies are similar for both conditions. For the second mode, the polar moment of inertia changes as nominal thick disk has smaller diameter than nominal disk. Although both conditions have similar mass, the smaller disk reduces the distance of second moment of mass from the spinning axis. Hence, this condition increases the natural frequency of the nominal thick disk as compared to that of the nominal disk.

Table 7: First mode natural frequency of shaft system with different disk mass

Disk mass	Natural frequency, Hz 4DOF	Natural frequency, Hz 5DOF	Differences (%)
Nominal	102.21	102.24	0.0
Heavy	88.08	88.09	0.0
Nominal thick	102.22	102.24	0.0

Table 8: Second mode natural frequency of shaft system with different disk mass

Disk mass	Natural frequency, Hz 4DOF	Natural frequency, Hz 5DOF	Differences (%)
Nominal	228.18	229.03	0.4
Heavy	220.32	221.12	0.4
Nominal thick	231.42	232.33	0.4

Figure 6 and Figure 7 depict the Campbell diagrams for the first and second whirling frequency, respectively, for three different disk masses modelled using the 4DOF and 5DOF models. Referring to Figure 6, the first vibration frequency mode corresponds to the 5DOF model changes greatly with the increase of speed as compared to the first vibration frequency of the 4DOF model. However, for the second mode, both 4DOF and 5DOF models show similar changes of FF and BF as the rotating speed increases. This occurs for each disk mass. Table 9 and Table 10 show the effect of disk mass towards critical speed., in which the nominal and nominal thick disk give slightly similar critical speed for the first and second modes. Due to more added mass in heavy disk, the whirling speed is lower compared to that of the nominal disk. The differences between the 4DOF and 5DOF models are significant for the first mode that gives the highest difference of 5.3% in the FF of the nominal thick disk. The lowest difference of 3.4% is for BF of heavy disk. Similar frequencies are obtained for nominal and nominal thick disks since both have similar mass with different geometry. However, as the mode of frequency increases to second mode, significance of torsional motion is decreasing with the highest difference of 1.6% is for FF of nominal thick disk. These results show that torsional motion needs to be considered in studying the effect of attaching disk with different mass, at least for the lowest mode of whirling frequency estimation. As the degree of mode increases, the torsional motion becomes less significant.

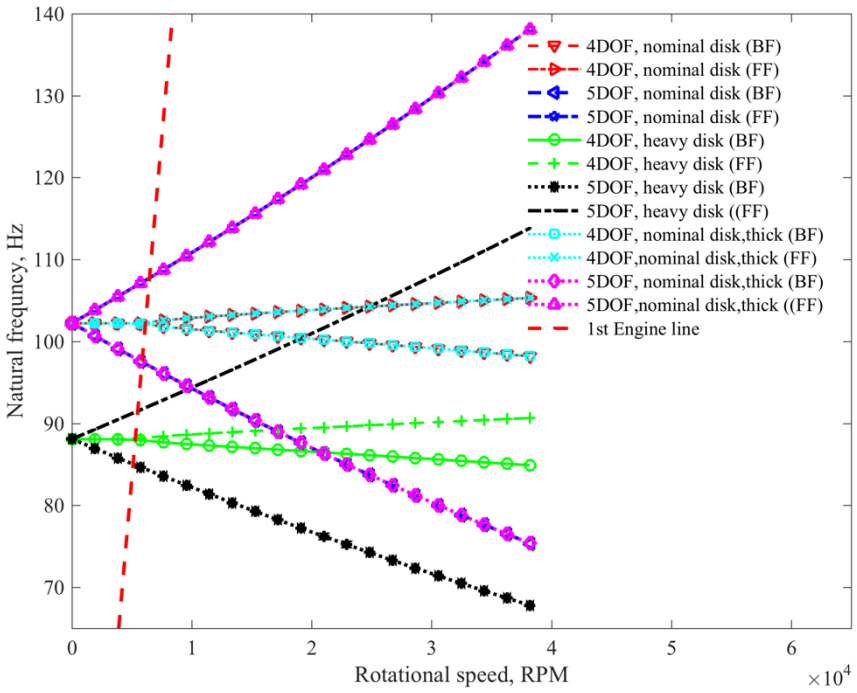

Figure 6: Effect of disk mass on the first mode of whirling frequency of shaft

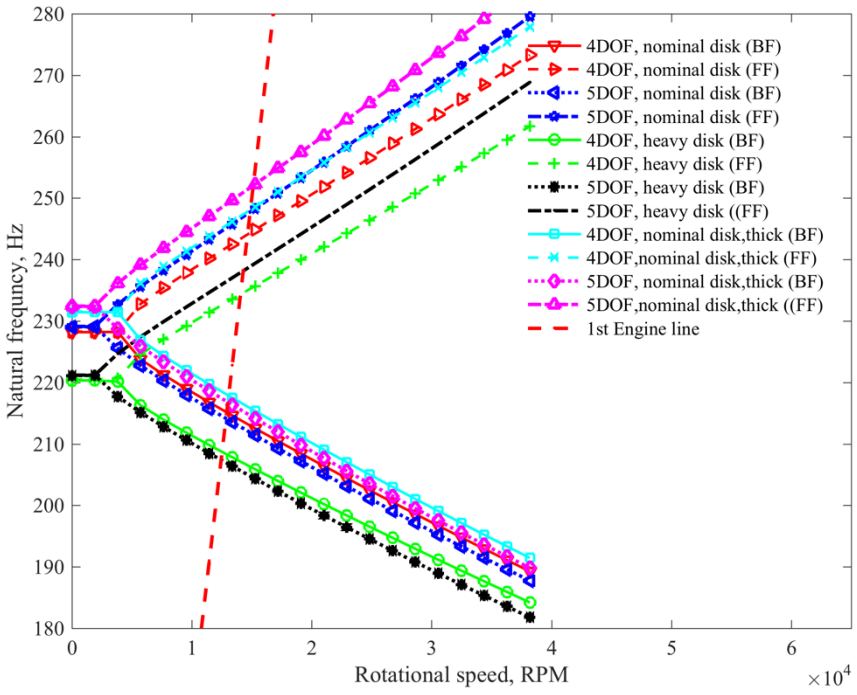

Figure 7: Effect of disk mass on the second mode of whirling frequency of shaft

Table 9: Comparison of whirling speed for different disk mass at first mode

Disk mass	**Whirling direction**	**Whirling speed, RPM 4DOF**	**Whirling speed, RPM 5DOF**	**Differences, %**
Nominal	BF	6140	5854	-4.66
	FF	6147	6465	5.17
Heavy	BF	5290	5109	-3.42
	FF	5296	5491	3.68
Nominal, thick	BF	6143	5857	-4.66
	FF	6145	6470	5.29

Table 10: The comparison of whirling speed for different disk mass at 2nd mode

Disk mass	**Whirling direction**	**Whirling speed, RPM 4DOF**	**Whirling speed, RPM 5DOF**	**Differences, %**
Nominal	BF	12920	12840	-0.62
	FF	14660	14860	1.36
Heavy	BF	12530	12460	-0.56
	FF	14070	14290	1.56
Nominal, thick	BF	13090	13010	-0.61
	FF	14910	15150	1.61

Last but not least, the effect of the number of disk attached to shaft on its free vibration is studied. Three disks with similar mass are added one after another into the shaft system. The disk is located at the same distance from each other. Figure 8 and Figure 9 show the plots of the first natural frequency mode against the rotational speed of the shafts having 1, 2 and 3 disks, respectively, using the 4DOF and 5DOF models. The plots show a big difference between the 4DOF and 5DOF models with regards

to FF and BF frequencies at the same value of speed. The 5DOF model shows much wider difference between the FF and BF frequencies as the speed increases. However, the difference between the 4DOF and the 5DOF models in terms of critical speed is less as shown in Table 11 and Table 12. Table 11 shows that the maximum difference between the 5DOF and the 4DOF models is 14%.

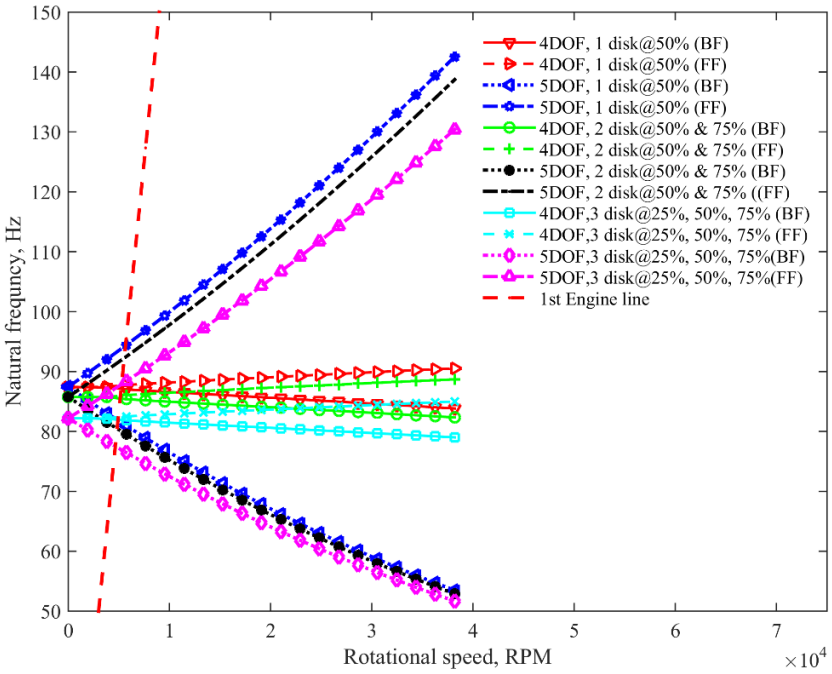

Figure 8: Effect of the number of disks on the first mode whirling frequency of shaft

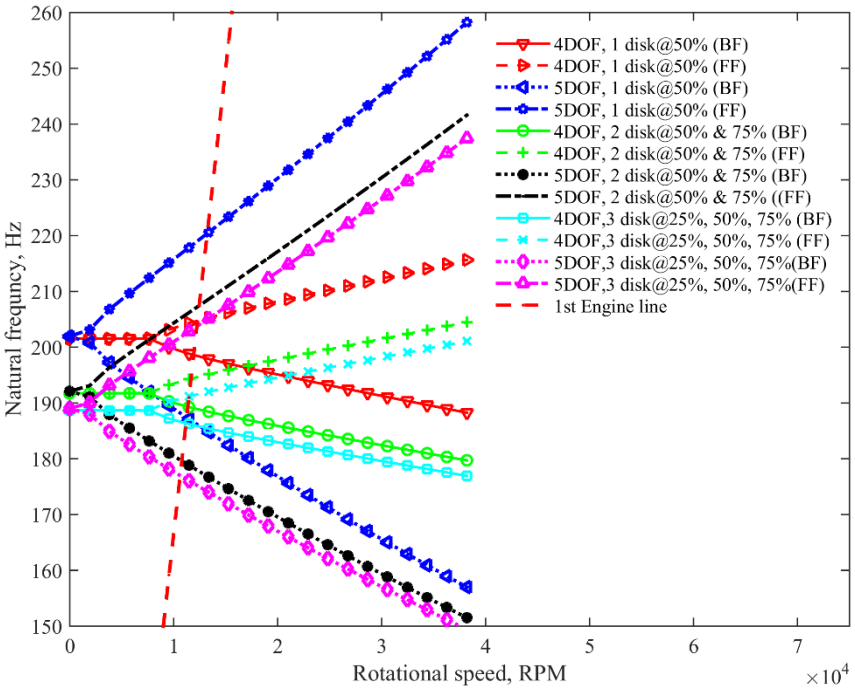

Figure 9: Effect of the number of disks on the second mode whirling frequency of shaft

Table 11: First mode of whirling speed for shaft having different number of disks

Disk quantity	Whirling direction	Whirling speed, RPM 4DOF	Whirling speed, RPM 5DOF	Differences, %
1	BF	5223	4908	-6.03
	FF	5262	5663	7.62
2	BF	5128	4832	-5.77
	FF	5175	5539	7.03
3	BF	4918	5651	14.90
	FF	4947	5281	6.75

Table 12: Second mode of whirling speed for shaft having different number of disks

Disk quantity	Whirling direction	Whirling speed, RPM 4DOF	Whirling speed, RPM 5DOF	Differences, %
1	BF	11910	11240	-5.63
	FF	12290	13230	7.65
2	BF	11350	10780	-5.02
	FF	11670	12440	6.60
3	BF	11180	10630	-4.92
	FF	11480	12230	6.53

4. Conclusion

A study has been conducted on the effect of disk parameters on the whirling frequency of high speed shaft while considering the torsional effect of the shaft. Finite element formulation in the form of the Mathieu-Hill type of equation is developed. The Bolotin's method is applied to obtain the quadratic eigenvalues equation that gives the Campbell's diagram. Some of the findings from this study include the effect of the location and mass of the disk on the natural frequency of shaft in static condition. In addition, it is also found that changing the geometry of the disk while maintaining its mass gives no effect to the natural frequency. The natural frequency of the shaft is lower for disk located at the centre of the shaft. Furthermore, the effect of torsional motion considered in the 5DOF model is significant as reflected by the wide difference between the FF and BF of the shaft. The difference in critical speed corresponding to 4DOF and 5DOF models highlights the importance to consider the torsional motion in studying the whirling frequency of the shaft with added disks.

Acknowledgement

The authors acknowledge the support in this study from Malaysia-Japan Institute of Technology and Universiti Teknologi Malaysia through the provision of the GUP Tier 2 Grant – PY/2017/00768.

References

[1] Pei Y C 2009 *European Journal of Mechanics and Solids* **28** 891–6
[2] Gerada D, Mebarki A, Brown N L, Gerada C, Cavagnino A and Boglietti A *IEEE Trans. Ind. Electron* **61** 2946–59
[3] Silber S, Sloupensky J, Dirnberger P, Moravec M, Amrhein A and Reisinger M *IEEE Trans. Ind. Electron* **61** 2990–7
[4] Crescimbini F, Lidozzi A, Calzo L and Solero G 2014 *IEEE Trans. Ind. Electron* **61** 2998–3011
[5] Tenconi A, Vaschetto S and Vigliani A 2014 *IEEE Trans. Ind. Electron* **61** 3022–9
[6] Ambekar A G 2006 *Mechanical Vibration and Noise Engineering* PHI Learning Pvt. Ltd.
[7] Lien-Wen C. and Der-Ming K 1991 *Comput. Struct.* **40** 741–7
[8] Karunendiran S and Zu J W 1999 *J. Vib. Acoust.* **121** 256–8
[9] Hosseini S A A and Zamanian M 2013 *Scientia Iranica* **20** 131-40
[10] Shahgholi M, Khadem S E and Bab S 2014 *Mech. Mach. Theory* **82** 128–40

[11] Wang S, Wang Y, Zi Y and He Z 2015 *J. Sound Vib.* **359** 116–35
[12] Jalali M H, Ghayour M, Ziaei-Rad S and Shahriari B 2014 *Measurement* **53** 1–9
[13] Seshendra K V S and Rao S B 2012 *Int. J. Mech. Appl.* **2** 10–13
[14] Nelson H D 1980 *J. Mech. Des.* **102** 793
[15] Bolotin V 1964 *The Dynamic Stability of Elastic Systems* Holden−Day
[16] Rao J S 2011 *Finite Element Methods for Rotor Dynamics* in *History of Rotating Machinery Dynamics* Springer Netherlands